

# Retinotopic Changes in the Gray Matter Volume and Cerebral Blood Flow in the Primary Visual Cortex of Patients With Primary Open-Angle Glaucoma

Shaodan Zhang,<sup>1,2</sup> Bo Wang,<sup>3</sup> Yuan Xie,<sup>4</sup> SenHua Zhu,<sup>3</sup> Ravi Thomas,<sup>5,6</sup> Guoping Qing,<sup>4</sup> Chun Zhang,<sup>1</sup> and Ningli Wang<sup>4</sup>

<sup>1</sup>Department of Ophthalmology, Peking University Third Hospital, Beijing, China

<sup>2</sup>Department of Ophthalmology, The 4th People's Hospital of Shenyang, Shenyang Eye Research Institute, Key Laboratory of Ophthalmology of Shenyang, Shenyang, Liaoning Province, China

<sup>3</sup>State Key Laboratory of Brain and Cognitive Science, Institute of Biophysics, Chinese Academy of Sciences, Beijing, China

<sup>4</sup>Beijing TongRen Eye Center, Beijing TongRen Hospital, Capital Medical University, Beijing, China

<sup>5</sup>Queensland Eye Institute, Brisbane, Australia

<sup>6</sup>University of Queensland, Brisbane, Australia

Correspondence: Chun Zhang, Department of Ophthalmology, Peking University Third Hospital, No. 49 Huayuanbei Street, Haidian District, Beijing 100191, China; zhangc1@yahoo.com. Ningli Wang, Beijing TongRen Eye Center, Beijing TongRen Hospital, Capital Medical University, No. 8, ChongWenMenNei Street, Chong-Wen District, Beijing 100730, China; wningli@vip.163.com.

SZ and BW contributed equally to the work presented here and should therefore be regarded as equivalent authors.

Submitted: May 17, 2015

Accepted: August 9, 2015

Citation: Zhang S, Wang B, Xie Y, et al. Retinotopic changes in the gray matter volume and cerebral blood flow in the primary visual cortex of patients with primary open-angle glaucoma. *Invest Ophthalmol Vis Sci*. 2015;56:6171–6178. DOI:10.1167/ iovs.15-17286

**PURPOSE.** To assess the cortical structure and cerebral blood flow changes in the brain of patients with primary open-angle glaucoma (POAG).

**METHODS.** High-resolution anatomical magnetic resonance imaging (MRI) and arterial spin labeling (ASL)-MRI were performed in 23 POAG patients and 29 controls. Patients were further divided into early-moderate and advanced groups based on mean deviation (MD) cutoff of 12 dB. A baseline scan was obtained and repeated during visual stimulation to the central preserved visual field in the more affected eye of POAG patients and a randomly selected eye of controls. Gray matter volume (GMV) and cerebral blood flow (CBF) throughout the whole brain were compared between patients and controls.

**RESULTS.** Compared to controls, a region with significant reduction of GMV was detected in the anterior calcarine fissure of advanced POAG patients ( $P < 0.001$ , voxels = 503, 1698 mm<sup>3</sup>). Patients with early-moderate POAG had resting CBF similar to that of controls. However, a region with marked CBF decrease was detected in the anterior calcarine fissure of advanced POAG patients ( $P < 0.001$ , voxels = 1687, 13,496 mm<sup>3</sup>). The region with CBF reduction in advanced POAG showed good colocalization with the region with GMV decrease in this group. Following visual stimulation, patients with advanced POAG showed significantly lower increase in CBF in the occipital lobes ( $P < 0.001$ , voxels = 112, 896 mm<sup>3</sup>) as compared to controls ( $P < 0.001$ , voxels = 1880, 15,040 mm<sup>3</sup>) and early-moderate POAG ( $P < 0.001$ , voxels = 2233, 17,864 mm<sup>3</sup>).

**CONCLUSIONS.** Primary open-angle glaucoma patients demonstrate a disease severity-dependent retinotopic pattern of cortical atrophy and CBF abnormalities in the visual cortex. Cerebral blood flow may be a potential biomarker for the brain involvement in glaucoma.

**Keywords:** primary open-angle glaucoma (POAG), gray matter volume (GMV), cerebral blood flow (CBF), magnetic resonance imaging (MRI), arterial spin labeling (ASL)

**G**laucoma comprises a group of diseases characterized by progressive retinal ganglion cell (RGC) loss, resultant optic nerve head changes, and visual field loss and is a major cause of irreversible blindness worldwide.<sup>1</sup> Intraocular pressure (IOP)-dependent and independent factors such as immune disturbance and vascular dysregulation have been implicated in the onset and progression of this disease.<sup>2,3</sup> More recently, several independent studies have provided evidence for the involvement of central visual targets in glaucoma. Marked neuronal degeneration and glial activation have been confirmed in the lateral geniculate nucleus (LGN) and visual cortex of nonhuman primates as well as human patients with glaucoma.<sup>4–12</sup> Atrophy of the optic nerve, optic chiasm, optic tract, LGN, optic radiation, and visual cortex associated with longstanding retinal visual field defects in glaucoma has also been demonstrated in

vivo using magnetic resonance imaging (MRI).<sup>4,13–16</sup> These changes in the brain may directly perturb processing of visual information or lead to further RGC loss and visual field defects through neurotrophic factor deprivation.<sup>17</sup> With advances in modern neuroimaging techniques, early detection and in vivo monitoring of the morphologic and functional changes in the human brain are possible and provide tools and opportunities for further investigation and understanding of the involvement of the brain in glaucoma. In the central nervous system (CNS), neurons and vascular cells form a functionally integrated network that is collectively termed the neurovascular unit. Alterations of the activity of the neurons may evoke dilation or constriction of neighboring blood vessels to regulate local blood flow perfusion.<sup>18</sup> Accordingly, cerebral blood flow (CBF) may be a potential indicator for the brain neuropathy in

glaucoma. In a previous study we reported an insufficiency in the hemodynamics in the posterior cerebral artery (PCA) of patients with primary open-angle glaucoma (POAG).<sup>19</sup> In the present study, we further investigate the structural and CBF changes in the brain of POAG patients using high-resolution anatomical MRI and arterial spin labeling (ASL) perfusion MRI.

## METHODS

### Subjects

Primary open-angle glaucoma patients between 40 and 60 years of age were enrolled from Beijing Tongren Eye Center and Department of Ophthalmology, Peking University Third Hospital. The diagnosis of POAG was based on an IOP more than 21 mm Hg, open anterior chamber angle, and glaucomatous abnormalities of the optic nerve head with correlating visual field defects. The relatively young age was chosen to reduce the risk of a confounding effect of aging on the brain structure and cerebrovascular system. Age- and sex-matched controls were recruited by advertising the research project.

All participants underwent a comprehensive ophthalmologic examination, including visual acuity, refraction, Goldman applanation tonometry, slit-lamp biomicroscopy, gonioscopy, ophthalmoscopy, and nonmydriatic retinal photography. Visual fields were assessed using the Humphrey 30-2 SITA standard program (Carl Zeiss Meditec, Dublin, CA, USA) and retinal nerve fiber layer (RNFL) thickness was measured using optical coherence tomography (OCT; Carl Zeiss Meditec). All subjects had a best-corrected visual acuity of 20/40 or better; a spherical refraction within  $\pm 5$  diopters (D) and cylinder correction within  $\pm 3$  D were permitted. All patients had established visual field defects with at least the central 5° or more preserved visual field in both eyes. Patients were further divided into an early-moderate and an advanced glaucoma group based on a mean deviation (MD) value in the visual field of their more affected eye. Those with MD  $\geq -12$  dB were classified as early-moderate glaucoma while those with MD  $< -12$  dB were grouped as advanced glaucoma. Patients with nonglaucomatous optic neuropathy, any retinopathy, opaque media, and ocular diseases that could affect the visual field were excluded, as were those with cardiovascular diseases, CNS diseases, and any conditions or symptoms that precluded MRI scanning.

The study adhered to the tenets of the Declaration of Helsinki and was approved by the ethics committee of the Peking University Third Hospital; informed consent was obtained from all patients.

### Magnetic Resonance Imaging

Magnetic resonance imaging was performed using a Trio 3.0 Tesla scanner (Siemens, Erlangen, Germany) with a 12-channel receiver head coil. During testing, subjects lay supine in the MRI scanner with two pieces of foam supporting the head to minimize movement. Whole-brain high-resolution T<sub>1</sub>-weighted anatomic scans were acquired with a four-echo magnetization-prepared rapid gradient-echo imaging (MPRAGE) sequence (TR = 2530 ms, TE = 1.64/3.5/5.36/7.22 ms, FOV = 256 × 256 mm<sup>2</sup>, matrix = 256 × 256).

Arterial spin labeling perfusion MRI, which uses magnetically labeled arterial water as an endogenous tracer to obtain quantified CBF maps, was performed with a pseudo-continuous arterial spin labeling (pCASL) sequence (single-shot gradient-echo echo-planar imaging, TR = 4000 ms, TE = 9.2 ms, FOV = 220 × 220 mm<sup>2</sup>, matrix = 64 × 64, and in-plane resolution = 3.4 × 3.4 mm<sup>2</sup>; 20 slices acquired in ascending

order with a slice thickness = 5 mm and a 1-mm gap between slices; labeling duration = 1650 ms; post labeling delay = 1200 ms; and numbers of controls/labels = 41 pairs). Scanning was initially performed with both eyes of the subject covered with an opaque occluder, and a total of 64 echo-planar imaging (EPI) images were obtained in a 4.5-minute scan. Next, a 3° checkerboard reversing at 8 Hz was presented to central preserved upper or lower hemifield of the eye with the more severe visual field loss (Fig. 1). The eye and the choice of central upper or lower hemifield to be tested in the control group were selected at random. The temporal frequency of the contrast-reversing checkerboard (8 Hz) was selected as it is reported to elicit a maximum blood oxygen level-dependent (BOLD) response from V1.<sup>20–24</sup> Refractive error of the tested eye was corrected with lenses fixed on the goggle; the fellow eye was covered with an occluder attached to the goggle. Computer-generated stimuli were back projected on a screen that was located inside the MRI bore near the patient's head. The subjects were asked to fixate a cross at the center of the screen, viewed at a total path length of 60 cm through a mirror situated above their eyes. The session lasted for 4.5 minutes. Image acquisition was started 4 to 6 seconds after the onset of the visual stimuli presentation, and a total of 64 EPI images were obtained.

### Data Analysis

**Voxel-Based Morphometry (VBM) Analysis.** Automated VBM analysis was conducted with VBM8 (<http://dbm.neuro.uni-jena.de/vbm/> [in the public domain]), which is an external toolbox of the SPM8 software package (<http://www.fil.ion.ucl.ac.uk/spm/software/spm8/> [in the public domain]). Voxel-based morphometry analysis assumes that each voxel of a T<sub>1</sub>-weighted high-resolution MR image contains a mixture of gray matter (GM), white matter (WM), and cerebrospinal fluid (CSF). The image is segmented to yield the content or probability of each tissue class at the voxel level. After transforming each individual brain image into the same stereotactic space, these voxel-based tissue probabilities can be statistically compared between different populations to determine local alterations of brain structure.<sup>25</sup> In brief, for each subject, the high-resolution structural image was first segmented into different brain tissue including GM, WM, and CSF and then normalized into standard Montreal Neurological Institute (MNI) space (voxels resampled to isotropic 1.5 × 1.5 × 1.5-mm<sup>3</sup>) with the standard routine provided by VBM8. The resulting images were visually checked to ensure that there were no misclassifications; the modulated normalized GM images that represented gray matter volume (GMV) images were then smoothed using a Gaussian filter with a 6-mm full width at half-maximum (FWHM) kernel. Finally, the group difference between the patients and controls of GMV were examined voxel-wise using the two-sample *t*-test model in SPM with sex and age of subjects added to the model as covariates. Areas of the brain that demonstrated significant differences between groups were thresholded at  $P < 0.001$  (cluster size  $\geq 40$ ) and visualized in SPM with pseudo-color. These detected regions were then looked up in the normalized human brain by referring to the Automated Anatomical Labeling (AAL) system (<http://www.cyceron.fr/index.php/en/plateforme-en/freeware> [in the public domain]) system.

**ASL Data Processing.** Traditional image preprocessing was carried out using SPM8 software for the ASL perfusion data. Specifically, after abandoning the first two pairs of EPI maps obtained in ASL scan to eliminate the effect of the inhomogeneous magnetic field, perfusion images were realigned and resliced to correct for head motion and mean volume created. Subjects whose head motion exceeded 2.0

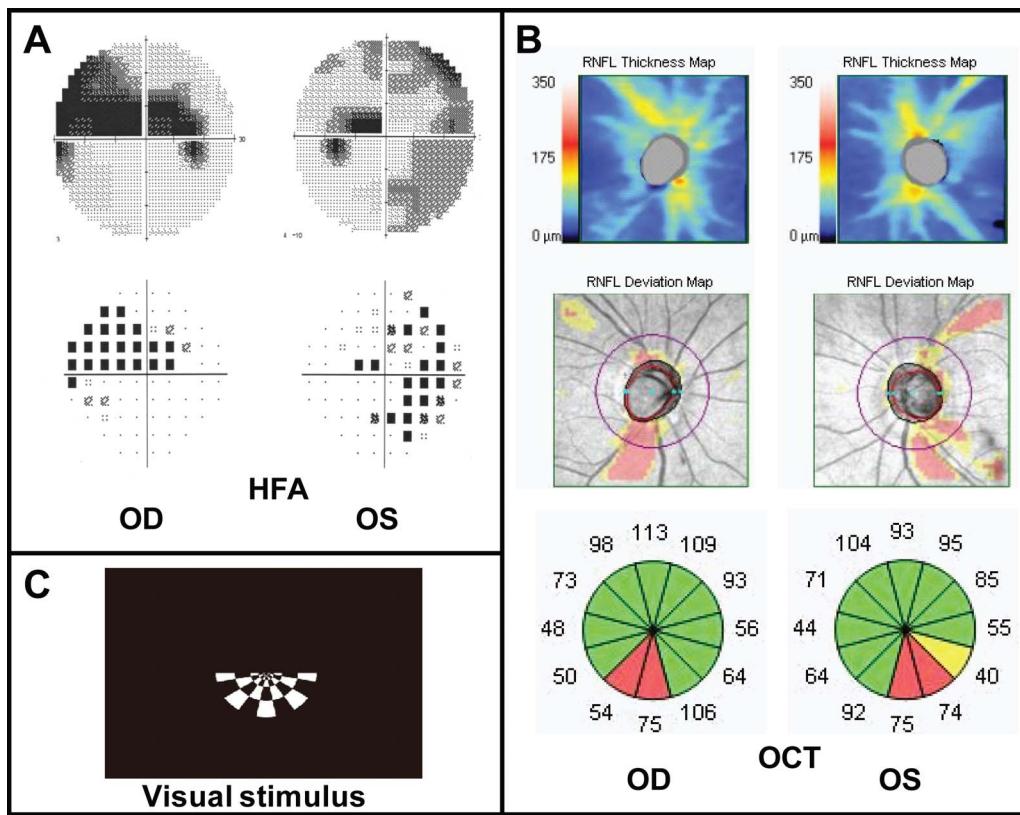


**FIGURE 1.** Visual field and optical coherence tomography measurements of a primary open-angle glaucoma (POAG) patient. (A) Humphrey Field Analyzer (HFA) 30-2 program revealed bilateral visual field defect in this patient. (B) Optical coherence tomography examination illustrated retinal nerve fiber layer (RNFL) thinning in the inferior temporal retina in both eyes. (C) According to the pattern of visual field loss in this patient, hemifield black and white reversing checkerboard was presented to the preserved central inferior visual field of the right eye. OD, right eye; OS, left eye.

mm or rotation exceeded  $2.0^\circ$  during scanning were excluded. Structural images were coregistered with the mean volume of functional images and subsequently smoothed using an 8-mm FWHM isotropic Gaussian kernel in SPM8. Cerebral blood flow images of the whole brain were then reconstructed from preprocessed perfusion images using Grocer toolbox (<http://www.fil.ion.ucl.ac.uk/spm/ext/#Grocer> [in the public domain]). The acquired CBF images were normalized to standard MNI space and the voxels resampled to isotropic  $2 \times 2 \times 2$ -mm $^3$ . The mean CBF maps of patients (both early-moderate and advanced POAG) as well as controls obtained both at rest and during visual stimulation were modeled in a  $2 \times 2$  factorial design with SPM. In order to eliminate the baseline difference of CBF across subjects, global mean scaling was done using the proportional normalization method in the generalized linear model (GLM). In line with the procedure done for the GMV analysis, the brain areas showing significant difference in the CBF between groups were also thresholded at  $P < 0.001$  (cluster size  $\geq 40$ ). The visualization and name labeling of the detected regions were done as in the VBM analysis. Global mean CBFs of controls and patients were also extracted with the global mean extraction tool provided in the Grocer toolbox.

## RESULTS

Twenty-three POAG patients, 14 males and 9 females with a mean age of  $47 \pm 7$  years, completed the study. Nine patients were defined as early-moderate glaucoma and 14 as advanced

glaucoma. The mean MD in the more and less affected eye was  $-18.6 \pm 9.6$  and  $-10.4 \pm 7.2$  dB, respectively. Twenty-nine healthy volunteers (19 males and 10 females, mean age  $48 \pm 7$  years) were recruited as controls. Distribution of age ( $t = -0.730$ ,  $P = 0.469$ ) and sex ( $\chi^2 = -0.119$ ,  $P = 0.732$ ) was comparable between glaucoma patients and controls.

## Changes in Gray Matter Volume in the Primary Visual Cortex of POAG Patients

Compared to controls, POAG patients showed significantly reduced GMV in the anterior part of the calcarine fissure, the region corresponding to the approximate anatomical projection zone of the peripheral visual field loss (Fig. 2A,  $P < 0.001$  uncorrected, cluster size  $\geq 40$ , voxels = 102, 344 mm $^3$ ). On analyzing the early-moderate and advanced glaucoma groups, a statistically significant GMV decrease was noticed only in the anterior calcarine fissure of advanced POAG patients (Fig. 2C,  $P < 0.001$  uncorrected, cluster size  $\geq 40$ , voxels = 503, 1698 mm $^3$ ). No GMV decrease was detected anywhere in the brain in the early-moderate glaucoma group. A small region with increased GMV was observed in the cuneus of early-moderate POAG patients compared with controls (Fig. 2B,  $P < 0.001$  uncorrected, cluster size  $\geq 40$ , voxels = 143, 483 mm $^3$ ).

## Resting Cerebral Blood Flow in the Primary Visual Cortex of POAG Patients

At baseline, the mean CBF in POAG patients ( $42.18 \pm 1.49$  mL/100 g/min) was similar to that in controls ( $41.89 \pm 1.71$  mL/

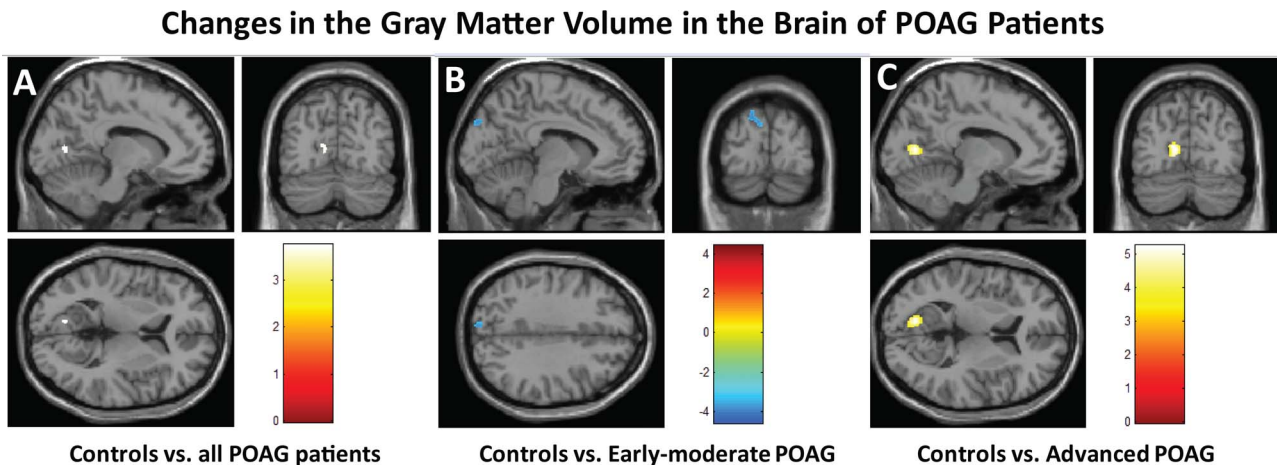


**FIGURE 2.** Changes in the gray matter volume (GMV) in POAG patients. Colors indicate statistically significant difference in GMV, with *yellow* indicating GMV decrease and *blue* indicating GMV increase in POAG patients compared with controls. (A) Gray matter volume reduction was detected in the anterior part of calcarine fissure in patients with POAG. (B) Gray matter volume increase was detected in the cuneus in early-moderate POAG patients compared with controls. (C) Region with significant GMV reduction was detected in the anterior calcarine fissure in advanced POAG patients compared with controls.

100 g/min) (independent 2-sample *t*-test,  $P = 0.898$ ) (Fig. 3A). An isolated regional decrease in CBF was detected in the anterior part of the calcarine fissure of glaucoma patients (Fig. 3B,  $P < 0.001$  uncorrected, cluster size  $\geq 40$ , voxels = 438, 3504 mm $^3$ ). No CBF changes could be detected anywhere in the brains of the early-moderate POAG group. A significant decrease in CBF was demonstrated in the anterior calcarine fissure in advanced glaucoma (Fig. 3C,  $P < 0.001$  uncorrected, cluster size  $\geq 40$ , voxels = 1687, 13,496 mm $^3$ ). This brain region with decreased CBF in the advanced glaucoma group showed good colocalization with the region of decreased GMV (Fig. 3D).

### Reduced Visual Evoked Cerebral Blood Flow in the Occipital Lobe of POAG Patients

When receiving monocular checkerboard stimulation, both controls and POAG patients showed significantly increased CBF in bilateral occipital poles as compared to their own baselines (Figs. 4A, 4B). Voxels with increased CBF after visual stimulation were significantly less in advanced POAG patients (Fig. 4D,  $P < 0.001$  uncorrected, cluster size  $\geq 40$ , voxels = 112, 896 mm $^3$ ) than in controls (Fig. 4A,  $P < 0.001$  uncorrected, cluster size  $\geq 40$ , voxels = 1880, 15,040 mm $^3$ ) and early-moderate POAG patients (Fig. 4C,  $P < 0.001$  uncorrected, cluster size  $\geq 40$ , voxels = 2233, 17,864 mm $^3$ ).

### DISCUSSION

We report a retinotopic reduction in the GMV and resting CBF in the anterior calcarine fissure, the region corresponding to the brain projection zone of peripheral visual field defect, in patients with advanced POAG. This is also the first report of compromised cerebral blood perfusion response in the occipital poles to visual stimulation presented to the central preserved “normal” visual field in patients with advanced POAG. These findings provide further evidence for the brain neurodegeneration in glaucoma and provide new evidence for the involvement of the cerebrovascular system in the pathophysiology of glaucoma. This highlights the potential use of CBF as an indicator for the detection of brain changes in glaucoma.

Atrophy of the visual cortex in glaucoma patients has been demonstrated in several studies. Our results are consistent with the MRI reports of Yu et al.<sup>26</sup> and Bogorodzki et al.<sup>27</sup> of local cortical atrophy in the primary visual cortex of patients with glaucoma. Boucard et al.<sup>13</sup> also reported a similar GM density decrease in the anterior part of the calcarine fissure in glaucoma patients, as well as in the occipital poles of those with age-related macular degeneration (AMD), who typically suffer from central visual field loss. In patients with dementia but without glaucoma, retinal neuronal damage as reflected by thinning of the ganglion cell-inner plexiform layer (GC-IPL) is associated with GM loss in the occipital and temporal lobes.<sup>28</sup> The data consistently respect the topographical relationship between brain involvement and retinal neurodegeneration.<sup>29</sup>

We detected regional GMV decrease in the anterior calcarine fissure of advanced POAG but not in early-moderate POAG. This is in agreement with a recent report of GM density changes in advanced, but not early POAG.<sup>30</sup> Yu et al.<sup>26</sup> documented significant differences in calcarine cortical thickness between mild and advanced glaucoma. Decreased cortical thickness was detected in the V5/MT+ area in patients with early glaucoma, while in advanced cases it was present in both V5/MT+ and anterior subregions of V1.<sup>31</sup> This finding is consistent with the concept that the magnocellular pathway may be affected earlier than the parvocellular pathway in glaucoma.<sup>12</sup> Although a primary neurodegenerative process in the brain cannot be excluded, the retinotopic and disease severity-related cortical changes in glaucoma suggest a type of secondary anterograde transsynaptic degeneration, or cortical plasticity, primed by the death of RGCs and absence of stimulation from the areas of visual field defects in glaucoma. Neurodegeneration in the visual cortex either may represent a state of “dormancy” or may actively participate in the disease progress through deprivation of brain-derived neurotrophic factors.<sup>17</sup> In recent years, a retinal prosthesis system (RPS) has been under development as a potentially valuable aid for restoring functional vision in those suffering from partial or total blindness.<sup>32</sup> It provides retinal stimulation and transmits the signal via normal visual pathway to the visual cortex. Patients with late-stage glaucoma, as well as other retinal degenerative diseases, may benefit from the visual prosthesis; but whether the brain atrophy in glaucoma could compromise the effect of RPS needs further investigation. Findings in the central visual targets in glaucoma may change its concept as an

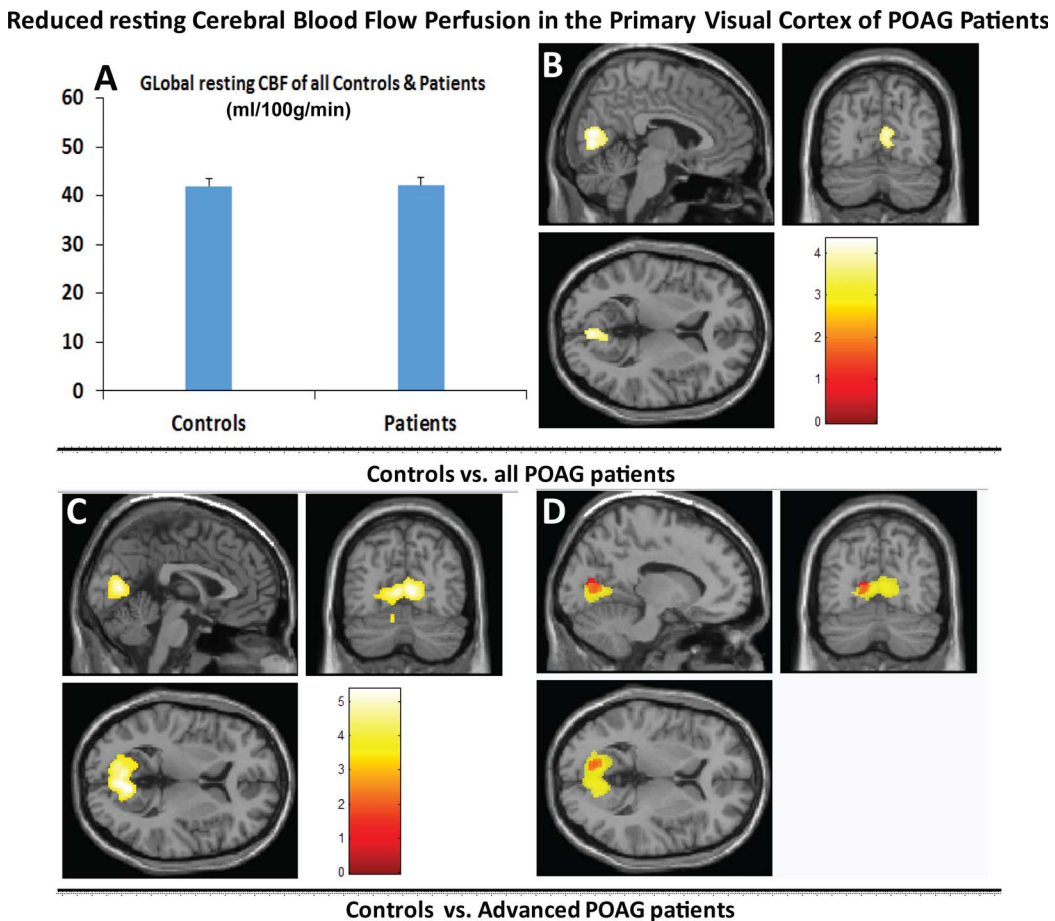


**FIGURE 3.** Comparison of the resting cerebral blood flow (CBF) perfusion between POAG patients and controls. **(A)** Comparable global mean CBF between POAG patients and controls at baseline. **(B)** Region with CBF reduction (yellow) in the anterior part of calcarine fissure in POAG patients. **(C)** Region with significant CBF reduction (yellow) in the anterior part of calcarine fissure in advanced POAG patients. **(D)** Overlay of the region with decreased CBF (yellow) with that with decreased gray matter volume (GMV) (red) in advanced glaucoma patients.

eye disease into a whole visual pathway neurodegenerative condition and may affect our clinical practice in the future.

We found a small region with increased GMV in the cuneus (Brodmann area, BA17) of early-moderate POAG patients. The cuneus is a small lobe in the occipital lobe that receives visual information from contralateral superior retina and projects fibers to the extrastriate cortex. A GMV increase in the cuneus may represent a compensation or replasticity of the visual cortex following early visual field loss in glaucoma. Cortical replasticity and cross-model plasticity have been widely observed in the brain of glaucoma patients.<sup>30,33,34</sup> Consistent with our present results, Williams et al.<sup>33</sup> previously reported that patients with glaucoma may have volumetric gains in some structures early in disease, but that brain volumes decrease toward and in some cases below control volumes as the disease progresses. Li et al.<sup>30</sup> reported significantly decreased GMV in the lingual gyrus, calcarine gyrus, postcentral gyrus, superior frontal gyrus, inferior frontal gyrus, and rolandic operculum of both sides, the right inferior occipital gyrus, left paracentral lobule, right supramarginal gyrus, and right cuneus in POAG patients. Increased GMV was detected in bilateral middle temporal gyrus, inferior parietal gyrus, angular gyrus, and left superior parietal gyrus, left precuneus, and the left middle occipital gyrus in these patients.<sup>30</sup> In another study, GM density reduction was located bilaterally in the primary visual cortex (BA17 and BA18) and paracentral lobule (BA5), right precentral gyrus (BA6), right middle frontal gyrus (BA9), right

inferior temporal gyrus (BA20), right angular gyrus (BA39), left praecuneus (BA7), left middle temporal gyrus (BA21), and superior temporal gyrus (BA22) while increased GM density was found in BA39. Altered integrity of WM tracts and brain atrophy was detected in both visual cortex and other distant nonvisual regions.<sup>34</sup> Differences between studies could be due to heterogeneity of patient groups or the different image processing and averaging techniques employed. The data are, however, consistent with the occurrence of cortical replasticity in the brain of patients affected by glaucoma, a phenomenon that merits further investigation.

Our results support the notion that established neurodegeneration in the brain may be a late-onset event in glaucoma.<sup>8</sup> Considering the role that brain changes may play in the process of disease progression, biomarkers that can specifically and sensitively reflect the brain changes in glaucoma may be useful in disease evaluation and follow-up. In the CNS, changes in the function, structure, or metabolism of neurons may lead to disturbance of the local CBF through neurovascular coupling.<sup>18,19,35</sup> We hypothesized that glaucomatous neurodegeneration in the brain may be accompanied by cerebral vascular deficiency. Cerebrovascular insufficiency in glaucoma has been reported by a few previous clinical studies, and includes abnormal CBF patterns, diffuse WM lesions, lacunar infarcts, and hemodynamic disturbances in the middle cerebral artery (MCA).<sup>36–43</sup> We have previously reported insufficiency in the hemodynamics and vasoreactivity of the PCA, the main

### Visual Stimulation Evoked Cerebral Blood Flow Increase in the Primary Visual Cortex of Controls and POAG Patients

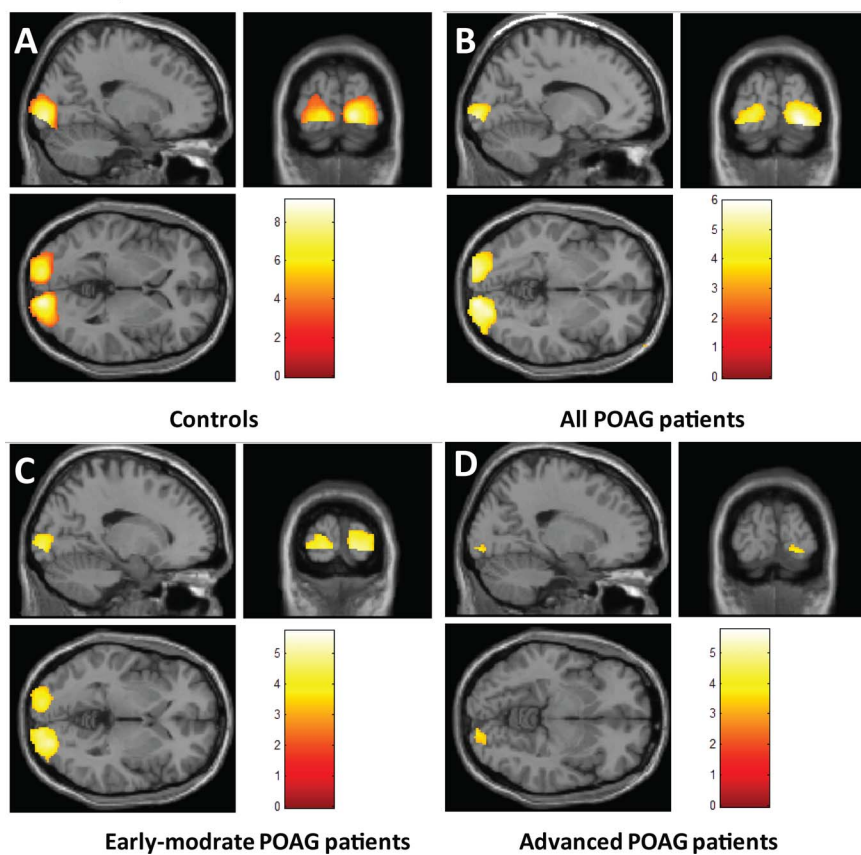


**FIGURE 4.** Visual evoked cerebral blood flow (CBF) perfusion changes in controls and POAG patients. (A) Significant CBF increase in bilateral occipital poles of controls (yellow). (B) Significant CBF increase in bilateral occipital poles of POAG patients (yellow). (C) Significant CBF increase in bilateral occipital poles of early-moderate POAG patients (yellow). (D) Small region with weak CBF increase in the left occipital pole of advanced POAG patients (yellow).

supplying vessel of the posterior visual pathways, in POAG.<sup>19</sup> A recent study reported reduction in the resting CBF in the primary visual cortex and its correlation with the loss of visual function in patients with POAG.<sup>44</sup> These findings are evidence of widespread involvement of the cerebrovascular system in glaucoma. It has, however, remained unclear whether and how cerebral vascular changes contribute to the brain neurodegeneration in glaucoma. The excellent colocalization of GMV decrease and resting CBF reduction in the peripheral visual field projection zones in the anterior calcarine fissure of advanced POAG in the present study supports our hypothesis of the role of neurovascular coupling in the brain changes that occur in glaucoma.

In addition to glaucoma, disturbances of CBF or cerebrovascular reactivity have also been widely observed in patients with Parkinson's disease, Alzheimer's disease, and multiple sclerosis.<sup>45–47</sup> These findings suggest a common involvement of the neurovascular mechanism in neurodegenerative diseases of the CNS. Dysregulated cerebrovascular reactivity may lead to unstable oxygen supply to local neurons, and may actively participate in the acceleration of neurodegeneration in the brain of the patients. Investigations of the cerebrovascular system may provide new insight into the pathogenesis of brain changes in glaucoma.

The new finding in the present study is the decreased CBF response to central visual stimulation in advanced POAG. Despite the preserved central visual field in the stimulated

region and normal GMV in bilateral occipital poles, patients with advanced POAG showed significantly compromised CBF changes in the occipital poles in response to central visual stimulation. This result is consistent with our previous publication of decreased vasoreactivity in bilateral PCAs to a reversing checkerboard stimulation presented to the central preserved "normal" visual field in patients with POAG.<sup>19</sup> In an earlier functional MRI study, a 5° hemifield reversing checkerboard was presented monocularly to the central apparently "normal" visual field of patients with asymmetric POAG. A significant decrease in blood oxygenation level-dependent (BOLD) signal changes was observed in the occipital poles when evoked by the glaucomatous eyes as compared to the contralateral, less affected fellow eye.<sup>10</sup> These and current findings suggest that disruption in cerebral vascular responses or cerebral blood perfusion may precede cortical structural changes, as well as detectable visual field defects in POAG. There may be a functional decrease in visual processing even in the visual field we defined as the "normal" central area in POAG. It has been reported that 25% to 35% of RGCs are lost prior to detectable abnormality in automated visual field testing.<sup>48</sup> A flow-on effect of early perceptual loss may be involved in the visual evoked cerebrovascular or CBF perfusion insufficiency in glaucoma. A mechanism involving neurovascular coupling cannot be excluded, as cortical neurons in the occipital poles of advanced POAG patients may be functionally inhibited or impaired. Decreased neuronal activity in this

region may disrupt the regulation of local arterioles and result in impaired visual evoked cerebrovascular responses. Future studies should examine the value of using CBF as a biomarker for the diagnosis and prediction of brain alterations in glaucoma.

There are several limitations to our study. First, to avoid the effect of aging on the cerebral vascular system, only patients between 40 to 60 years of age without a history of cardiovascular disease were included. Our findings can be extrapolated only to similar patients without systemic vascular dysregulation, the presence of which may have a (currently unknown) effect on the CBF in glaucoma. Second, although SPM-based automated volumetric analysis is considered an acceptable substitute for labor-intensive manual estimates,<sup>49</sup> manual delineation-based volumetric assessment is traditionally regarded as the gold standard for intracranial volumetric analysis in brain degeneration.<sup>25,49</sup> The use of the gold standard method might make the results a little bit different. Third, we compared the GMV and CBF between POAG patients and controls across the whole brain, and only regions showing significant differences between groups under a specific threshold were referred to the Automated Anatomical Labeling system of normalized human brain for localization. We consider this a first step in exploring the mechanism of CNS involvement related to glaucoma. Investigation of the structural and cerebrovascular alterations in separated visual cortex areas (e.g., V1/V2/V3 areas) would provide valuable information.

In summary, this is the first report of a colocalized reduction in the GMV and resting CBF in the brain projection zone of glaucomatous visual field defects in advanced POAG. This finding partly supports neurovascular coupling as a mechanism of brain involvement in glaucoma. More importantly, the occipital poles of advanced POAG patients that showed GMV and resting CBF perfusion comparable with that of early-moderate glaucoma patients and controls, demonstrated significantly decreased CBF response to monocular visual stimulation presented to the central apparently "unaffected" visual field. This raises the possibility of using CBF as an index for the evaluation of central visual function or for detection of brain changes in patients with glaucoma. Glaucoma provides a model for the study of "neurovascular coupling mechanism" in CNS neurodegenerative diseases. Whether patients with POAG may benefit from neuroprotective therapies directed at the entire visual pathway or at improving the regulation of cerebral vasoreactivity in addition to conventional strategies for lowering intraocular pressure is speculative.

### Acknowledgments

Supported by National Nature Science Foundation of China Grants 81100661 and 91132302, Ministry of Science and Technology of China Grant 2012CB825505, Postdoctoral Science Foundation of China Grant 20100480170, and Key Lab Open Foundation of Capital Medical University Grant 2010YK SJ04. The authors alone are responsible for the content and writing of the paper.

**Disclosure:** **S. Zhang**, None; **B. Wang**, None; **Y. Xie**, None; **S. Zhu**, None; **R. Thomas**, None; **G. Qing**, None; **C. Zhang**, None; **N. Wang**, None

### References

- Quigley HA, Broman AT. The number of people with glaucoma worldwide in 2010 and 2020. *Br J Ophthalmol*. 2006;90:262-267.
- Huang P, Qi Y, Xu YS, et al. Serum cytokine alteration is associated with optic neuropathy in human primary open angle glaucoma. *J Glaucoma*. 2010;19:324-330.
- Resch H, Garhofer G, Fuchsjager-Mayrl G, Hommer A, Schmetterer L. Endothelial dysfunction in glaucoma. *Acta Ophthalmol*. 2009;87:4-12.
- Chen WW, Wang N, Cai S, et al. Structural brain abnormalities in patients with primary open-angle glaucoma: a study with 3T MR imaging. *Invest Ophthalmol Vis Sci*. 2013;54:545-554.
- Crawford ML, Harwerth RS, Smith EL III, Shen F, Carter-Dawson L. Glaucoma in primates: cytochrome oxidase reactivity in parvo- and magnocellular pathways. *Invest Ophthalmol Vis Sci*. 2000;41:1791-1802.
- Crawford ML, Harwerth RS, Smith EL III, Mills S, Ewing B. Experimental glaucoma in primates: changes in cytochrome oxidase blobs in V1 cortex. *Invest Ophthalmol Vis Sci*. 2001;42:358-364.
- Dai H, Morelli JN, Ai F, et al. Resting-state functional MRI: functional connectivity analysis of the visual cortex in primary open-angle glaucoma patients. *Hum Brain Mapp*. 2013;34:2455-2463.
- Gupta N, Ang LC, Noel de Tilly L, Bidaisee L, Yucel YH. Human glaucoma and neural degeneration in intracranial optic nerve, lateral geniculate nucleus, and visual cortex. *Br J Ophthalmol*. 2006;90:674-678.
- Weber AJ, Chen H, Hubbard WC, Kaufman PL. Experimental glaucoma and cell size, density, and number in the primate lateral geniculate nucleus. *Invest Ophthalmol Vis Sci*. 2000;41:1370-1379.
- Qing G, Zhang S, Wang B, Wang N. Functional MRI signal changes in primary visual cortex corresponding to the central normal visual field of patients with primary open-angle glaucoma. *Invest Ophthalmol Vis Sci*. 2010;51:4627-4634.
- Zhang S, Wang H, Lu Q, et al. Detection of early neuron degeneration and accompanying glial responses in the visual pathway in a rat model of acute intraocular hypertension. *Brain Res*. 2009;1303:131-143.
- Yucel YH, Zhang Q, Weinreb RN, Kaufman PL, Gupta N. Effects of retinal ganglion cell loss on magnoc-, parvo-, koniocellular pathways in the lateral geniculate nucleus and visual cortex in glaucoma. *Prog Retin Eye Res*. 2003;22:465-481.
- Boucard CC, Hernowo AT, Maguire RP, et al. Changes in cortical grey matter density associated with long-standing retinal visual field defects. *Brain*. 2009;132:1898-1906.
- Dai H, Mu KT, Qi JP, et al. Assessment of lateral geniculate nucleus atrophy with 3T MR imaging and correlation with clinical stage of glaucoma. *AJNR Am J Neuroradiol*. 2011;32:1347-1353.
- Ramli NM, Sidek S, Rahman FA, et al. Novel use of 3T MRI in assessment of optic nerve volume in glaucoma. *Graefes Arch Clin Exp Ophthalmol*. 2014;252:995-1000.
- Hernowo AT, Boucard CC, Janssonius NM, Hooymans JM, Cornelissen FW. Automated morphometry of the visual pathway in primary open-angle glaucoma. *Invest Ophthalmol Vis Sci*. 2011;52:2758-2766.
- Johnson TV, Bull ND, Martin KR. Neurotrophic factor delivery as a protective treatment for glaucoma. *Exp Eye Res*. 2011;93:196-203.
- Zonta M, Angulo MC, Gobbo S, et al. Neuron-to-astrocyte signaling is central to the dynamic control of brain microcirculation. *Nat Neurosci*. 2003;6:43-50.
- Zhang S, Xie Y, Yang J, et al. Reduced cerebrovascular reactivity in posterior cerebral arteries in patients with primary open-angle glaucoma. *Ophthalmology*. 2013;120:2501-2507.
- De Yoe EA, Bandettini P, Neitz J, Miller D, Winans P. Functional magnetic resonance imaging (fMRI) of the human brain. *J Neurosci Methods*. 1994;54:171-187.
- Engel SA, Glover GH, Wandell BA. Retinotopic organization in human visual cortex and the spatial precision of functional MRI. *Cereb Cortex*. 1997;7:181-192.

22. Engel SA, Rumelhart DE, Wandell BA, et al. fMRI of human visual cortex. *Nature*. 1994;369:525.

23. Sereno MI, Dale AM, Reppas JB, et al. Borders of multiple visual areas in humans revealed by functional magnetic resonance imaging. *Science*. 1995;268:889–893.

24. Tootell RB, Hadjikhani NK, Vanduffel W, et al. Functional analysis of primary visual cortex (V1) in humans. *Proc Natl Acad Sci U S A*. 1998;95:811–817.

25. Callaert DV, Ribbens A, Maes F, Swinnen SP, Wenderoth N. Assessing age-related gray matter decline with voxel-based morphometry depends significantly on segmentation and normalization procedures. *Front Aging Neurosci*. 2014;6:124.

26. Yu L, Xie B, Yin X, et al. Reduced cortical thickness in primary open-angle glaucoma and its relationship to the retinal nerve fiber layer thickness. *PLoS One*. 2013;8:e73208.

27. Bogorodzki P, Piatkowska-Jankó E, Szaflik J, Szaflik JP, Gacek M, Grieb P. Mapping cortical thickness of the patients with unilateral end-stage open angle glaucoma on planar cerebral cortex maps. *PLoS One*. 2014;9:e93682.

28. Ong YT, Hilal S, Cheung CY, et al. Retinal neurodegeneration on optical coherence tomography and cerebral atrophy. *Neurosci Lett*. 2015;584:12–16.

29. Kaushik M, Graham SL, Wang C, Klistorner A. A topographical relationship between visual field defects and optic radiation changes in glaucoma. *Invest Ophthalmol Vis Sci*. 2014;55:5770–5775.

30. Li C, Cai P, Shi L, et al. Voxel-based morphometry of the visual-related cortex in primary open angle glaucoma. *Curr Eye Res*. 2012;37:794–802.

31. Yu L, Yin X, Dai C, et al. Morphologic changes in the anterior and posterior subregions of V1 and V2 and the V5/MT+ in patients with primary open-angle glaucoma. *Brain Res*. 2014;1588:135–143.

32. da Cruz L, Coler BF, Dorn J, et al. The Argus II epiretinal prosthesis system allows letter and word reading and long term function in patients with profound vision loss. *Br J Ophthalmol*. 2013;97:632–636.

33. Williams AL, Lackey J, Wizov SS, et al. Evidence for widespread structural brain changes in glaucoma: a preliminary voxel-based MRI study. *Invest Ophthalmol Vis Sci*. 2013;54:5880–5887.

34. Frezzotti P, Giorgio A, Motolese I, et al. Structural and functional brain changes beyond visual system in patients with advanced glaucoma. *PLoS One*. 2014;9:e105931.

35. Metea MR, Newman EA. Glial cells dilate and constrict blood vessels: a mechanism of neurovascular coupling. *J Neurosci*. 2006;26:2862–2870.

36. Harris A, Zarfati D, Zalish M, et al. Reduced cerebrovascular blood flow velocities and vasoreactivity in open-angle glaucoma. *Am J Ophthalmol*. 2003;135:144–147.

37. Harris A, Siesky B, Zarfati D, et al. Relationship of cerebral blood flow and central visual function in primary open-angle glaucoma. *J Glaucoma*. 2007;16:159–163.

38. Akarsu C, Bilgili YK, Unal B, Taner P, Ergin A, Kara SA. Cerebral hemodynamics in ocular hypertension. *Graefes Arch Clin Exp Ophthalmol*. 2005;243:317–320.

39. Ong K, Farinelli A, Billson F, Houang M, Stern M. Comparative study of brain magnetic resonance imaging findings in patients with low-tension glaucoma and control subjects. *Ophthalmology*. 1995;102:1632–1638.

40. Kitsos G, Zikou AK, Bagli E, Kosta P, Argyropoulou MI. Conventional MRI and magnetisation transfer imaging of the brain and optic pathway in primary open-angle glaucoma. *Br J Radiol*. 2009;82:896–900.

41. Sugiyama T, Utsunomiya K, Ota H, Ogura Y, Narabayashi I, Ikeda T. Comparative study of cerebral blood flow in patients with normal-tension glaucoma and control subjects. *Am J Ophthalmol*. 2006;141:394–396.

42. Stroman GA, Stewart WC, Golnik KC, Cure JK, Olinger RE. Magnetic resonance imaging in patients with low-tension glaucoma. *Arch Ophthalmol*. 1995;113:168–172.

43. Suzuki J, Tomidokoro A, Araie M, et al. Visual field damage in normal-tension glaucoma patients with or without ischemic changes in cerebral magnetic resonance imaging. *Jpn J Ophthalmol*. 2004;48:340–344.

44. Duncan RO, Sample PA, Bowd C, Weinreb RN, Zangwill LM. Arterial spin labeling fMRI measurements of decreased blood flow in primary visual cortex correlates with decreased visual function in human glaucoma. *Vision Res*. 2012;60:51–60.

45. Marshall O, Lu H, Brisset JC, et al. Impaired cerebrovascular reactivity in multiple sclerosis. *JAMA Neurol*. 2014;71:1275–1281.

46. Benedictus MR, Binnewijzend MA, Kuijer JP, et al. Brain volume and white matter hyperintensities as determinants of cerebral blood flow in Alzheimer's disease. *Neurobiol Aging*. 2014;35:2665–2670.

47. Al-Bachari S, Parkes LM, Vidyasagar R, et al. Arterial spin labelling reveals prolonged arterial arrival time in idiopathic Parkinson's disease. *Neuroimage Clin*. 2014;6:1–8.

48. Kerrigan-Baumrind LA, Quigley HA, Pease ME, Kerrigan DF, Mitchell RS. Number of ganglion cells in glaucoma eyes compared with threshold visual field tests in the same persons. *Invest Ophthalmol Vis Sci*. 2000;41:741–748.

49. Malone IB, Leung KK, Clegg S, et al. Accurate automatic estimation of total intracranial volume: a nuisance variable with less nuisance. *Neuroimage*. 2015;104:366–372.